Fibroblast growth factor 5 overexpression ameliorated lipopolysaccharide-induced apoptosis of hepatocytes through regulation of the phosphoinositide-3-kinase/protein kinase B pathway

Shengyu Cui[1,2,3], Yuhua Li[4], Xutao Zhang[1,2,3], Bing Wu[1,2,3], Ming Li[1,2,3], Jixian Gao[1,2,3], Lin Xu[5], Hao Xia[1,2,3]

[1]Department of Cardiology, Renmin Hospital of Wuhan University, Wuhan, Hubei 430060, China;
[2]Cardiovascular Research Institute, Wuhan University, Wuhan, Hubei 430060, China;
[3]Hubei Key Laboratory of Cardiology, Wuhan, Hubei 430060, China;
[4]Intensive Care Unit, Wuhan Children's Hospital (Wuhan Maternal and Child Healthcare Hospital), Tongji Medical College, Huazhong University of Science and Technology, Wuhan, Hubei 430019, China;
[5]Department of Geriatrics, Renmin Hospital of Wuhan University, Wuhan, Hubei 430060, China.

Abstract

Background: Sepsis is a systemic inflammatory syndrome induced by several infectious agents. Multiple organs are affected by sepsis, including the liver, which plays an important role in metabolism and immune homeostasis. Fibroblast growth factors (FGFs) participate in several biological processes, although the role of *FGF5* in sepsis is unclear.

Methods: In this study, lipopolysaccharide (LPS) was administrated to mice to establish a sepsis-induced liver injury. A similar *in vitro* study was conducted using L-02 hepatocytes. Western blot and immunohistochemistry staining were performed to evaluate the *FGF5* expression level in liver tissues and cells. Inflammatory cell infiltrations, cleaved-caspase-3 expressions, reactive oxygen species and levels of inflammatory cytokines were detected by immunofluorescence, dihydroethidium staining, and reverse transcription quantitative polymerase chain reaction analysis, respectively. Flow cytometry was used to detect the apoptosis level of cells. In addition, ribonucleic acid (RNA)-sequencing was applied to explore the possible mechanism by which *FGF5* exerted effects.

Results: LPS administration caused *FGF5* down-regulation in the mouse liver as well as in L-02 hepatocytes. Additionally, with *FGF5* overexpression, liver injury and the level of hepatocyte apoptosis were ameliorated. Further, RNA sequencing performed in hepatocytes revealed the phosphoinositide-3-kinase/protein kinase B (PI3K/AKT) pathway as a possible pathway regulated by *FGF5*. This was supported using an inhibitor of the PI3K/AKT pathway, which abrogated the protective effect of *FGF5* in LPS-induced hepatocyte injury.

Conclusion: The anti-apoptotic effect of *FGF5* on hepatocytes suffering from LPS has been demonstrated and was dependent on the activation of the PI3K/AKT signaling pathway.

Keywords: Apoptosis; *FGF5*; Hepatocyte; Liver; PI3K/AKT; Sepsis

Introduction

Sepsis, with high mortality, is a complex clinical syndrome caused by systemic inflammatory response, resulting in immune suppression and eventually leading to shock and multiple organs dysfunction.[1] The liver, as an important immune and metabolic organ, is often severely damaged during sepsis.[2] Liver injury caused by sepsis is attributed to pathological mechanisms such as liver microcirculation disorder, oxidation and antioxidant system imbalance, intestinal bacterial migration, and uncontrolled inflammatory response.[3] Liver dysfunction has a special prognostic correlation with sepsis and is a strong independent predictor of sepsis-induced mortality.[2,4] The current treatments for sepsis-induced liver injury mainly include anti-infection, extracorporeal liver support, and other basic treatments, although these treatments are still less effective for some patients. Therefore, understanding the underlying mechanism of liver injury in sepsis can provide a direction for future precise treatment.

Access this article online

Quick Response Code:

Website: www.cmj.org

DOI: 10.1097/CM9.0000000000002540

Correspondence to: Lin Xu, Department of Geriatrics, Renmin Hospital of Wuhan University. No. 99 Zhangzhidong Road, Wuchang District, Wuhan, Hubei 430060, China
E-Mail: linxu2018@whu.edu.cn;
Hao Xia, Department of Cardiology, Renmin Hospital of Wuhan University; Cardiovascular Research Institute, Wuhan University; Hubei Key Laboratory of Cardiology. No. 99 Zhangzhidong Road, Wuchang District, Wuhan, Hubei 430060, China
E-Mail: xiahao1966@163.com

Chinese Medical Journal 2022;135(23)

Received: 19-08-2022; **Online:** 02-01-2023 **Edited by:** Rongman Jia and Xiuyuan Hao

The fibroblast growth factor (FGF) superfamily consists of 22 members, of which FGF5 is a secreted signaling protein.[5-7] The FGFs participate in biological processes such as cardiovascular remodeling,[8-10] and pathological embryogenesis,[11,12] and exert complex effects on some diseases, including cancers.[13,14] However, in previous studies, *FGF5* seems to have received insufficient attention in areas other than hair growth.[15-17] Recently, a few studies suggested that *FGF5* played a regulatory role in non-alcoholic fatty liver disease,[18,19] but the specific mechanism is not fully understood. Therefore, given the possible role of *FGF5* in liver-related diseases, we conducted this study to investigate the effect of *FGF5* on sepsis-induced liver injury and discussed its possible mechanism. We demonstrated that *FGF5* overexpression protected the septic liver and confirmed that the phosphoinositide-3-kinase/protein kinase B (PI3K/AKT) signaling pathway was involved in the protective effect of *FGF5*.

Methods

Animals

Male C57BL/6 mice aged eight weeks were obtained from the Animal Experimental Center of Three Gorges University (Yichang, China). The mice were housed under specific pathogen-free conditions and had free access to food and water. All animal experiments in this study were approved by the Animal Experimental Center of Wuhan Third Hospital (ethical number: SY2022–010) and were conducted in accordance with the Guide for the Care and Use of Laboratory Animals published by the United States National Institutes of Health.

Model of acute liver injury

A mouse model of acute liver injury was established by a single intraperitoneal injection of LPS. Mice were intraperitoneally injected with LPS with a dose of 10 mg/kg and sacrificed 12 h after injection.[20,21] The mice were divided into four groups as follows: normal group, fed normally and treated with an injection of saline; LPS group, received an intraperitoneal injection of LPS (L2880, Sigma-Aldrich, St. Louis, MO, USA); LPS + adenovirus (Ad)-*FGF5* group, injected with *FGF5*-over-expressed Ad (Gene Chem Co. Ltd., Shanghai, China) intravenously (injected via the tail vein with 1×10^9 plaque-forming units per mouse) one week before the 12 h LPS stimulation;[22,23] and LPS + Ad-control group, injected with negative control adenovirus (Gene Chem Co. Ltd.) one week before the 12 h LPS stimulation.

Immunohistochemistry

Citrate antigen retrieval buffer (pH 6.0) (Pinuofei Biological Technology Co, Ltd., Wuhan, China) was used to retrieve the antigen of liver slices in the microwave. Then, the endogenous peroxidase in the tissue slices was blocked in a solution of 3% hydrogen peroxide. Next, the slices were incubated with 3% bovine serum albumin (Solarbio Life Science, Beijing, China) for 30 min, with an FGF5 antibody (1:200, Proteintech, Wuhan, China) overnight. Finally, the slices were stained with horseradish peroxidase-conjugated secondary antibody (Agilent Technologies, Santa Clara, CA, USA) for approximately 1 h at room temperature and with diaminobenzidine (Agilent Technologies) for 2–5 min at room temperature until a brown color developed. For cell samples, the cells were first grown on climbing slices and then subjected to immunohistochemical staining. The staining procedure was similar to that of the liver slices above.

Hematoxylin-eosin (HE) staining

Liver from the sacrificed mice in each group was freshly harvested and soaked in 4% paraformaldehyde for more than 24 h. The tissue samples were then dehydrated, embedded, sectioned, dewaxed, and stained with hematoxylin (nuclei staining) and eosin (cytoplasm staining), and the slides were finally observed under a microscope (Leica Microsystems, Weztlar, Hesse-Darmstadt, Germany).

Immunofluorescence

Immunofluorescence assay for the staining for F4/80 and cleaved-caspase-3 was used to assess the infiltration of inflammatory cells in the mouse liver tissue and apoptosis level of hepatocytes, respectively. Specifically, the paraffin sections were dewaxed in water, and the tissue sections were placed in a repair box filled with citric acid antigen repair buffer (pH 6.0) (Pinuofei Biological Technology Co, Ltd.), and the antigen retrieval was performed in a microwave oven. The sections were then blocked in 3% bovine serum albumin for approximately 30 min. Next, the sections were incubated with the relevant primary antibodies (F4/80 [1:200, Proteintech] and cleaved-caspase-3 [1:200, Abcam, Cambridge, UK]) overnight at 4°C to allow the binding of antigen to antibody. At the next day, the sections were incubated with secondary antibodies (1:500, Jackson, Pennsylvania, USA) at room temperature for 1 h, and 4′,6-diamidino-2-phenylindole (DAPI, 1:100, Solarbio) was used to stain the nuclei. The images were obtained through an immunofluorescence microscope system (NIKON, Tokyo, Japan).

Cell culture

L-02 cells of the human fetal hepatocyte line were purchased from the Cell Bank of the Chinese Academy of Sciences (Shanghai, China). Cells were maintained in high-glucose dulbecco's modified eagle medium (HyClone, Logan, Utah, USA) supplemented with 10% fetal bovine serum (BIOEXPLORER, Colorado, USA). Cells were incubated at 37°C with 5% CO_2. When the cell density reached about 70% in the six-well plate, the cells were transfected using Lipo8000^{TM} Transfection Reagent (C0533FT, Beyotime Biotechnology, Shanghai, China) with either a plasmid (3 μg)-carrying human *FGF5* gene (Gene Chem Co. Ltd.) or a control plasmid (3μg) (Gene Chem Co. Ltd.); 48 h after transfection, these cells were then stimulated using 100 ng/mL LPS for 24 h. In addition, a PI3K/AKT signaling inhibitor, LY294002 (20 μmol/L, MedChemExpress, NJ, USA) combined with LPS was administered simultaneously 48 h after cell transfection.

Determination of biochemical indexes

Blood was obtained by retro-orbital bleeding from anesthetized mice. Serum samples were collected after centrifugation and sent to the Laboratory Department of Renmin Hospital of Wuhan University for automated biochemical analysis. Alanine aminotransferase (ALT) and aspartate aminotransferase (AST) were detected to reflect liver function and liver injury.

Detection of reactive oxygen species (ROS) level

Intra-cellular ROS levels were detected using dihydroethidium reagent. Frozen liver slices and L-02 cells were successively stained with dihydroethidium (D7008, Sigma, for liver slices; S0063, Beyotime Institute of Biotechnology, for cells) and DAPI (C1002, Beyotime Biotechnology). Specifically, the liver slices were stained with dihydroethidium for 30 min and DAPI for 10 min; the cells were washed with serum-free culture medium and incubated with the 5 μmol/L dihydroethidium at 37°C for 30 min and the DAPI for 10 min. The images were obtained under a fluorescence microscope (NIKON).

Analysis of ribonucleic acid (RNA)-sequencing

Total RNA of L-02 cells from different groups was extracted using RNAiso Plus (TaKaRa, Kyoto, Japan) according to the manufacturer's instructions. After RNA was tested for purity, concentration, and integrity, only high-quality RNA sample was used to construct sequencing library; high-throughput RNA sequencing was performed by Majorbio (Shanghai, China). The data were analyzed on the online platform of Majorbio Cloud Platform (www.majorbio.com). P value <0.05 and >1.5 times difference in gene expression was considered statistically significant between the two groups.

Flow cytometry

The cultured cells were trypsinized and washed with phosphate-buffered saline, and then, the annexin binding buffer was added to resuspend the cells. After 15 min incubation with 5 μL Annexin V-Phycoerythrin (PE) (BD Biosciences, New York, NJ, USA) and 5 μL 7-amino-actinomycin D (BD Biosciences), the cells were analyzed by flow cytometry (NovoCyte, Palo Alto, CA, USA). The apoptotic rate was taken as the sum of early and late apoptosis.

Quantitative real-time polymerase chain reaction analysis (PCR)

RNAiso Plus (TaKaRa) was used to extract total RNA. Next, complementary DNA (cDNA) was synthesized by using Servicebio RT First Strand cDNA Synthesis Kit (Servicebio, Wuhan, China) according to the manufacturer's instructions. Real-time quantitative polymerase chain reaction was performed using Servicebio 2*SYBR Green qPCR Master Mix kit (Low ROX) (Servicebio) and ABI ViiA7 Real-Time PCR system (Applied Biosystems, MA, USA).

Western blot

Briefly, the proteins extracted from the livers and cells were separated by sodium dodecyl sulfate-polyacrylamide gel electrophoresis and then transferred to nitrocellulose filter membranes. After blocking in the protein-free rapid blocking buffer (Epizyme Biotech, Shanghai, China), the membranes were washed with tris-buffered saline + Tween 20 (TBST) for three times and incubated overnight with primary antibodies for FGF5 (1:500, Affinity Biosciences, Jiangsu, China), phosphorylated-PI3K (p-PI3K, 1:1000, Abcam), PI3K (p85, 1:1000, Abcam), phosphorylated-AKT (p-AKT; Ser473, 1:1000, Cell Signaling Technology, Danvers, MA, USA), AKT (1:1000, Cell Signaling Technology), B cell lymphoma-2 (BCL-2) (1:1000, Abcam), BCL2-associated X (BAX) (1:1000, Abcam), caspase-9 (1:1000, Abcam), cleaved-caspase-9 (1:1000, Abcam), caspase-3 (1:1000, Abcam), cleaved-caspase-3 (1:1000, Abcam), and glyceraldehyde-3-phosphate dehydrogenase (GAPDH) (1:1000, Cell Signaling Technology). The next day, the membranes were incubated with horseradish peroxidase-conjugated secondary antibody for 1 h at room temperature. Finally, the visualization of membranes was realized by enhanced chemiluminescence reagent and in a ChemiDoc XRS$^+$ system (BIO-RAD, Hercules, CA, USA). The gray value of protein was quantified by Image J software (National Institutes of Health, Bethesda, MD, USA).

Statistical analysis of data

All data in our study were analyzed through GraphPad Prism software (GraphPad Software, San Diego, California, USA). One-way analysis of variance (ANOVA) followed by Tukey *post hoc* test was performed when comparing multiple groups; while the comparison of differences in two groups was done by unpaired Student's t-test. The criterion for statistical significance was $P < 0.05$.

Results

FGF5 was down-regulated in liver cells exposed to LPS

We determined the levels of *FGF5* in normal livers and LPS-treated livers, and as shown in Figure 1A, 1C, and 1E, a significantly down-regulated level of FGF5 was revealed in livers exposed to LPS. Further, the same trend was also observed in L-02 cells treated with LPS *in vitro* [Figure 1B, 1D, and 1F].

Overexpression of FGF5 ameliorated liver injuries in vivo

Next, FGF5 was overexpressed in livers of mice by injecting an adenovirus carrying the *FGF5* gene [Figure 2A and 2B]. After LPS stimulation, the liver exhibited remarkable damage, characterized by the destruction of liver tissue structure [Figure 2C], abnormal elevations of liver enzymes [Figure 2D and 2E] and inflammatory cytokines [Figure 2J and 2K], obvious infiltration of inflammatory cells [Figure 2F and 2H], and increased ROS level [Figure 2G and 2I]. Interestingly, with FGF5 overexpression, these LPS-induced pathological changes in the liver were ameliorated compared to the negative control group [Figure 2C–K].

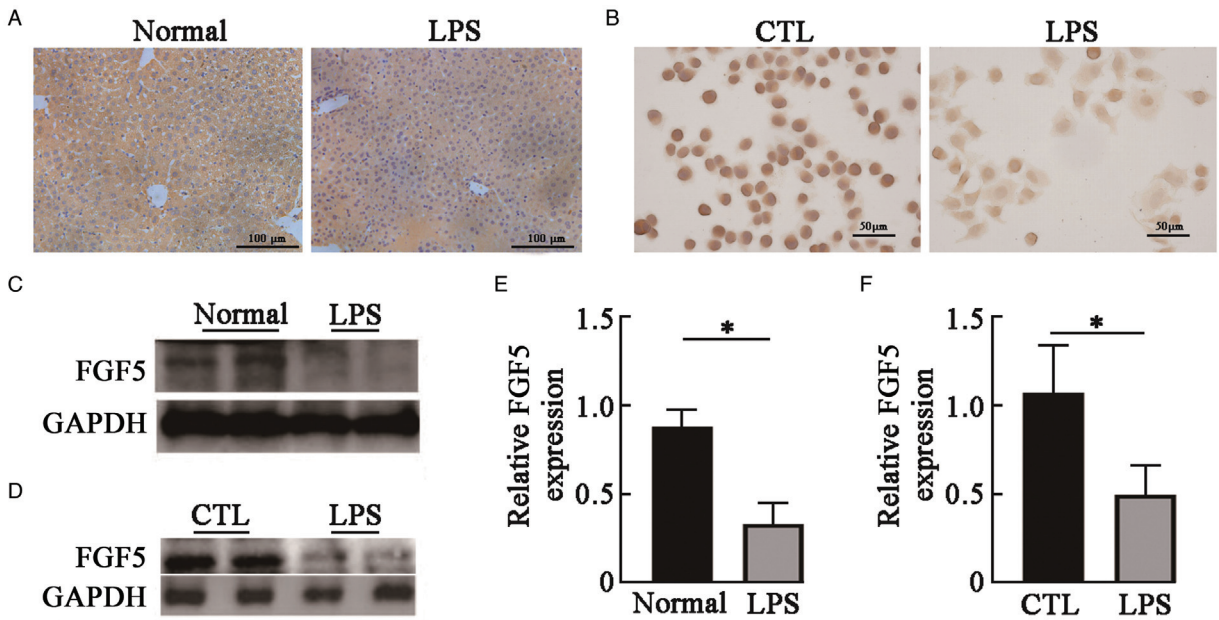

Figure 1: FGF5 is down-regulated in hepatocytes treated with LPS. (A) Representative images of liver immunohistochemical staining for FGF5. (B) Representative images of immunohistochemical staining for FGF5 in L-02 cells. (C, E) Expression of FGF5 in liver tissues detected by Western blot and its statistical analysis results displayed by a bar graph. (D, F) Expression of FGF5 in L-02 cells detected by Western blot and its statistical analysis results displayed by the bar graph. $n = 6$, $^{*}P < 0.05$. CTL: Control group; FGF5: Fibroblast growth factor 5; *GAPDH*: Glyceraldehyde-3-phosphate dehydrogenase; LPS: Lipopolysaccharide.

Overexpression of FGF5 relieved hepatocyte injuries in vitro

We performed an *in vitro* experiment to confirm the protective effects of FGF5 overexpression on hepatocytes. We used plasmids carrying *FGF5* gene to overexpress FGF5 in L-02 cells [Figure 3A–C]. As expected and similar to our animal results, LPS-stimulated cells showed an elevated ROS level compared with those in the control group, whereas FGF5-overexpressed cells showed decreased ROS levels compared with the negative control group [Figure 3D and 3E]. Further, flow cytometry [Figure 3H and 3I] results indicated that FGF5 overexpression in hepatocytes reduced LPS-induced cell apoptosis; immunofluorescence assay showed that the expression of cleaved-caspase-3 [Figure 3F and 3G] was also reduced after FGF5 overexpression. In conclusion, these results suggested that FGF5 overexpression reduced hepatocyte ROS levels and LPS-induced apoptosis.

PI3K/AKT signaling might account for the protective effects of FGF5

To elucidate the possible mechanism of *FGF5* ameliorating LPS-induced liver cell damage, we performed RNA sequencing to determine the possible signaling pathway through which *FGF5* may exert its action. A total of 453 differentially expressed genes were detected between the LPS + *FGF5*-plasmid and LPS + Control-plasmid groups, of which 204 genes were up-regulated and 249 genes were down-regulated in the LPS + *FGF5*-plasmid group. Subsequently, Kyoto Encyclopedia of Genes and Genomes (KEGG) enrichment was performed on these differentially expressed genes, and it was found that the PI3K/AKT signaling pathway was most significantly enriched [Figure 4A]. Therefore, the analysis of differentially expressed genes suggested that PI3K/AKT signaling was regulated by *FGF5*.

FGF5 affected PI3K/AKT and apoptotic pathways in vivo

Given that the enrichment analysis indicated that the PI3K/AKT signaling pathway might be involved in the protective effect of FGF5, we adopted the Western blot method to detect the activation of this pathway. As shown in Figure 4B–D, both p-PI3K and p-AKT were inhibited after LPS stimulation, whereas they were re-activated with FGF5 overexpression in the liver. Furthermore, reactivation of PI3K/AKT signaling was accompanied by decreased expression of pro-apoptotic proteins, including BAX, cleaved-caspase-9/caspase-9, and cleaved-caspase-3/caspase-3, and increased expression of anti-apoptotic proteins including BCL-2 [Figure 4B, 4E–H]. These results confirmed that *FGF5* indeed had a regulatory effect on the PI3K/AKT signaling pathway and might play an anti-apoptotic role by activating the PI3K/AKT signaling pathway in the liver.

FGF5 affected PI3K/AKT and apoptotic pathways in vitro

We also verified the regulation of PI3K/AKT signaling by *FGF5* using *in vitro* hepatocyte experiments. As depicted in Figure 5, our *in vitro* experiment confirmed the activation effect of *FGF5* on PI3K/AKT signaling and the inhibitory effect on apoptotic signals.

FGF5 protected hepatocytes against apoptosis via activating the PI3K/AKT pathway

To verify the anti-apoptotic effect of *FGF5* on liver cells through the activation of the PI3K/AKT signaling

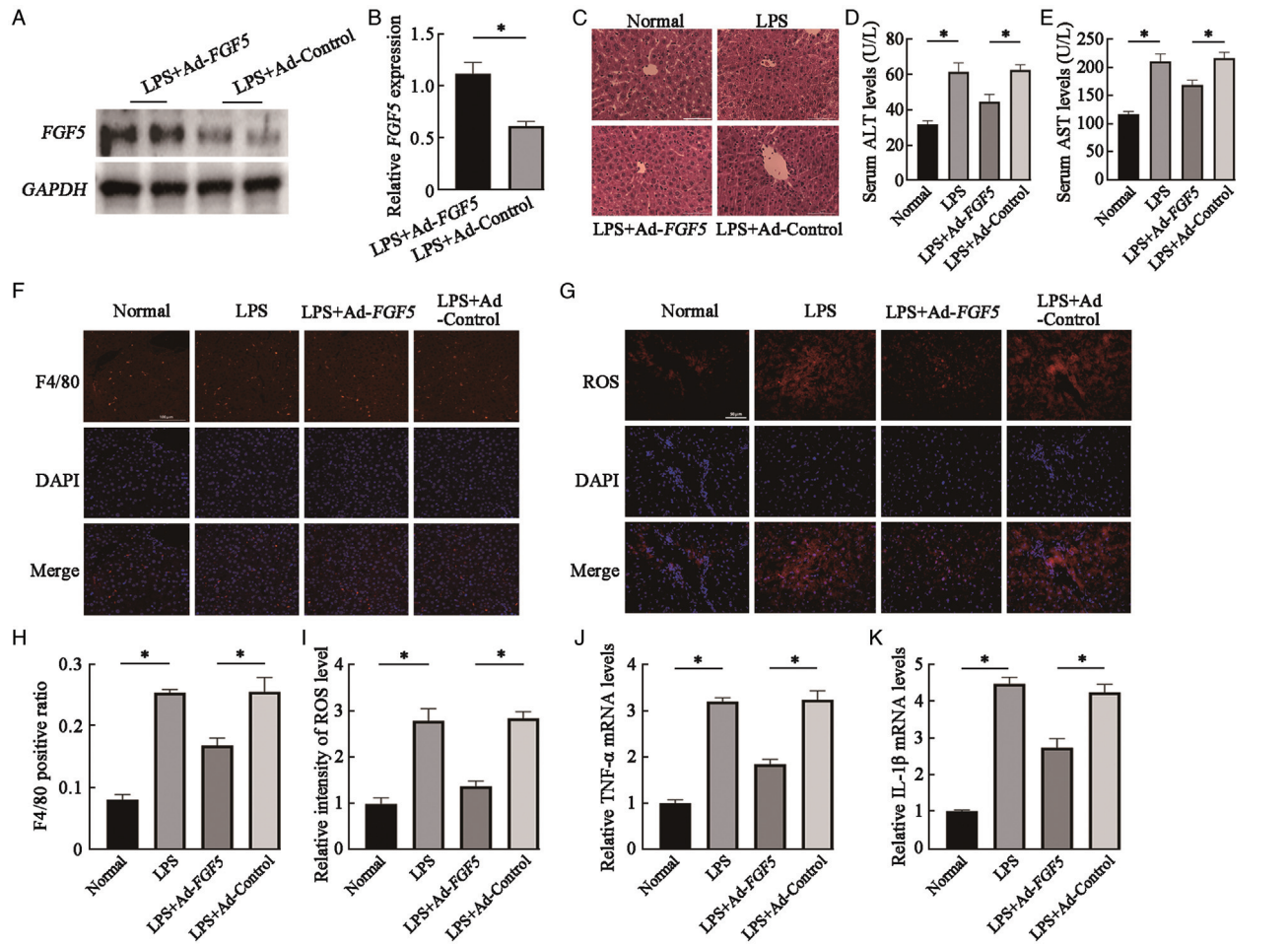

Figure 2: Overexpression of fibroblast growth factor 5 (FGF5) ameliorates liver injuries induced by LPS. (A, B) Representative blot images and corresponding statistical analysis graph reflecting the expressions of FGF5 in the liver ($n = 4$, $^{*}P < 0.05$). (C) Representative HE staining of liver from different groups. (D, E) The levels of ALT and AST in normal, LPS, LPS + Ad-*FGF5*, and LPS + Ad-control groups. (F, H) Representative immunofluorescence images of *F4/80* staining in livers and its statistical analysis ($n = 5$, $^{*}P < 0.05$). (G, I) Representative ROS staining of livers from different groups and its statistical analysis is shown in a bar graph ($n = 5$, $^{*}P < 0.05$). (J, K) Relative mRNA levels of TNF-α and IL-1β in livers ($n = 5$, $^{*}P < 0.05$). ALT: Alanine aminotransferase; AST: Aspartate transaminase; DAPI: 4′,6-diamidino-2-phenylindole; *GAPDH*: Glyceraldehyde-3-phosphate dehydrogenase; HE: Hematoxylin-eosin; IL-1β: Interleukin-1β; LPS: Lipopolysaccharide; LPS + Ad-control group: LPS + adenovirus-control group; LPS + Ad-*FGF5*: LPS + adenovirus-*FGF5* group; mRNA: Message RNA; ROS: Reactive oxygen species; TNF-α: Tumor necrosis factor-α.

pathway, we applied PI3K/AKT signaling inhibitor, LY294002, to the liver cells based on FGF5 overexpression. The protein results [Figure 6] showed that with the inhibition of PI3K/AKT signaling, the expression of pro-apoptotic proteins that had been down-regulated by FGF5 overexpression was increased and that of anti-apoptotic proteins that had been up-regulated by FGF5 overexpression was reduced; this meant that the anti-apoptotic effect of *FGF5* was abrogated with the suppression of PI3K/AKT signaling. Therefore, *FGF5* exerted an anti-apoptotic effect on hepatocytes by activating the PI3K/AKT signaling pathway, thus protecting hepatocytes from LPS-induced injury.

Discussion

Currently, there is a lack of clear diagnostic criteria for sepsis-related liver injury in clinical practice, and the incurrence mechanism is also unclear. As sepsis is usually accompanied by liver injury, it is of great significance to further study its pathogenesis and related treatment methods. In the current study, *FGF5* showed a protective effect against liver injury, which was reflected by its ability to reduce liver inflammation levels and improve hepatocyte apoptosis. Further, elucidating the mechanism by which *FGF5* exerted a protective effect in LPS-induced hepatic injury, the results of KEGG enrichment from RNA-sequence data showed that the PI3K/AKT signaling pathway was involved in the effect of *FGF5* on LPS-treated hepatocytes. Moreover, *FGF5* stimulated the activation of the PI3K/AKT signaling pathway, thereby relieving apoptosis and promoting hepatocyte survival, thus possibly serving as a mechanism to alleviate sepsis-induced liver injuries.

The *FGF* family contains more than 20 molecules and is widely involved in various biological processes.[24-26] A recent study has demonstrated that *FGF1* variant, a modified *FGF1*, is effective in preventing and reversing hepatic steatosis and steatohepatitis by activating adenosine 5′-monophosphate-activated protein kinase (AMPK), implicating the antioxidant function of *FGF*.[27] Similarly,

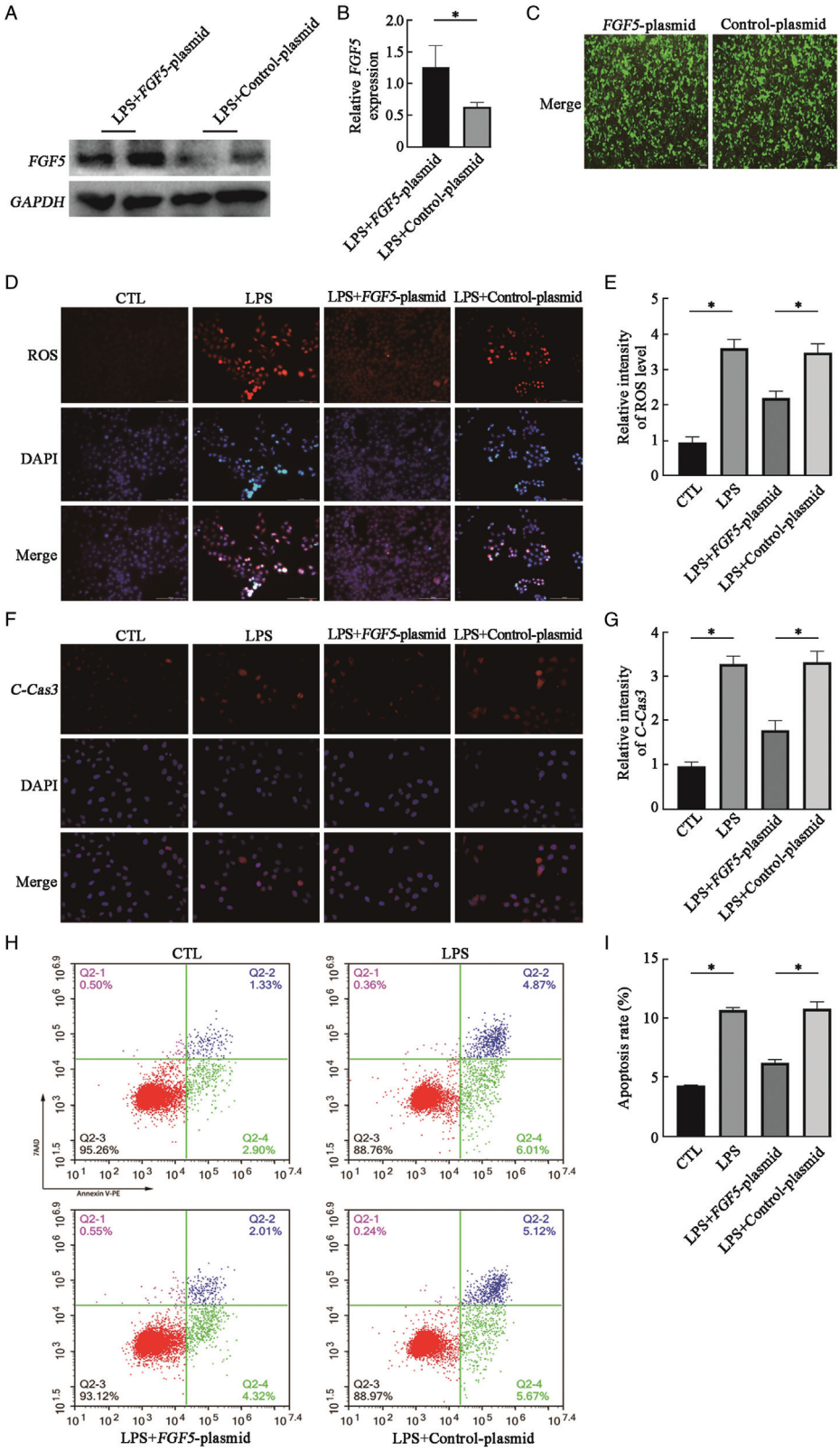

Figure 3: Overexpression of fibroblast growth factor 5 (*FGF5*) reduces LPS-induced hepatocyte injury *in vitro*. (A, B) Representative blot image and its corresponding statistical analysis graph reflecting the expression of *FGF5* in L-02 cells ($n = 4$, $^{*}P < 0.05$). (C) Merged fluorescent figures indicated the efficiency of plasmid transfection in L-02 cells. (D, E) Representative ROS staining of cells from different groups and its statistical analysis shown as a bar graph (×400, $n = 5$, $^{*}P < 0.05$). (F, G) Representative immunofluorescence image of cleaved-caspase-3 staining in livers and its statistical analysis ($n = 5$, $^{*}P < 0.05$). (H, I) Results of apoptosis rate assessed by flow cytometry and statistical analysis (×400, $n = 3$, $^{*}P < 0.05$). Annexin V-PE: Annexin V-Phycoerythrin; C-*cas3*: Cleaved-caspase 3; CTL: Control group; DAPI: 4′,6-diamidino-2-phenylindole; *GAPDH*: Glyceraldehyde-3-phosphate dehydrogenase; LPS: Lipopolysaccharide; ROS: Reactive oxygen species; 7AAD: 7-Aminoactinomycin D.

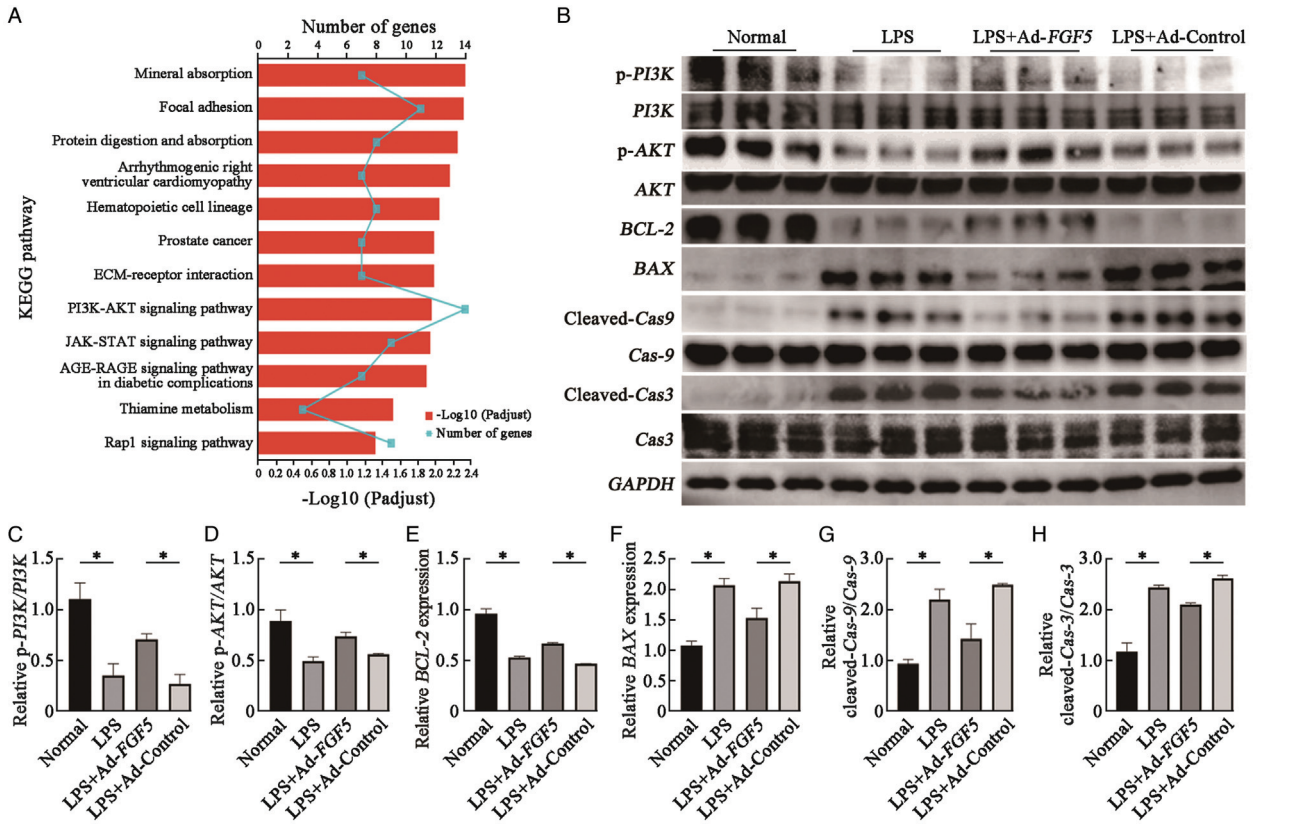

Figure 4: The protective effect of fibroblast growth factor 5 (*FGF5*) on LPS injury might be realized by regulating the phosphoinositide-3-kinase/protein kinase B (PI3K/AKT) pathway. (A) KEGGs enrichment analysis of the differentially expressed genes ($n = 3$, $P < 0.05$, and >1.5 times difference in gene expression was considered statistically significant between the two groups). (B) The PI3K/AKT and apoptotic pathways *in vivo*: Representative blot images. (C–H): The corresponding statistical analysis graphs. ($n = 3$, $^{*}P < 0.05$). AGE-RAGE: AGE-Receptor for AGE; *BAX*: B cell lymphoma-2 *(BCL2)*-associated X; *cas-3*: Caspase-3; *cas-9*: Caspase-9; DEGs: Different expression genes; ECM: Extra-cellular matrix; *GAPDH*: Glyceraldehyde-3-phosphate dehydrogenase; KEGG: Kyoto Encyclopedia of Genes and Genome; JAK-STAT: Janus kinase-signal transducers and activators of transcription; LPS: Lipopolysaccharide; LPS + Ad-control group: LPS + adenovirus-control group; LPS + Ad-*FGF5:* LPS + adenovirus-*FGF5* group; nosig: No significance; p-*AKT*: Phosphorylated-protein kinase B; p-*PI3K*: Phosphorylated-phosphoinositide-3-kinase; Rap1: *Ras*-related Protein 1.

FGF4[28] and *FGF21*[29-31] have also been found to exert protective and antioxidant effects on the fatty liver by activating the AMPK-mediated signaling axis. Thus, *FGF* family members show excellent antioxidant and anti-inflammatory abilities in some liver diseases. Additionally, FGFs also exert anti-apoptotic effects in other research fields.[32-36] For instance, Okada *et al*[32] have uncovered therapeutic effects of *FGF2* on reducing neuronal apoptosis through activation of PI3K/AKT signaling. However, there are few studies on *FGF5*, and the current reports on *FGF5* mainly focus on its regulation of hair growth.[15-17] Interestingly, a few previous studies have shown a potential link between *FGF5* and inflammation-related diseases: *FGF5* variance was reported to be associated with hypertension in humans,[37-40] and *FGF5* deletion was related to severe hepatic steatosis.[18,19] In a word, these studies support the protective role of *FGF5* in sepsis-related injury.

We constructed an adenovirus and a plasmid carrying the *FGF5* gene, which was then transferred into mice and L-02 cells. Excessive ROS production can lead to cell death, and reduced ROS often means lower levels of intra-cellular oxidative stress and better cellular status.[41] Our results indicated a protective effect of FGF5 overexpression on LPS-induced injury in hepatocytes, which was reflected by decreased ROS levels and the subsequent increased survival rate. To further reveal the protective mechanism of *FGF5*, RNA sequencing was carried out on a liver cell line after an *in vitro* experiment. KEGG enrichment analysis showed that the PI3K/AKT signaling pathway had the highest enrichment degree, suggesting that *FGF5* might play a protective role on hepatocytes through the regulation of the PI3K/AKT signaling pathway.

PI3K/AKT signaling has widely been considered a regulator of cell survival and anti-apoptosis signaling.[42,43] Most studies have demonstrated the beneficial effects of PI3K/AKT on cell injury induced by various factors,[44,45] and some have proposed the regulatory role of FGFs on PI3K/AKT signaling.[46-48] In our current study, LPS induced both hepatocyte apoptosis and inhibited the PI3K/AKT pathway; FGF5 overexpression led to increased PI3K and AKT phosphorylation, which indicated that following LPS stimulation, the activation of the PI3K/AKT pathway was FGF5 dependent. Further, FGF5 overexpression also reduced the apoptosis level in hepatocytes. To further verify that *FGF5* did exert an anti-apoptotic effect on hepatocytes through the PI3K/AKT signaling pathway, LY294002, a PI3K/AKT signaling inhibitor, was applied to cells *in vitro*, which inhibited the anti-apoptotic effect of *FGF5*.

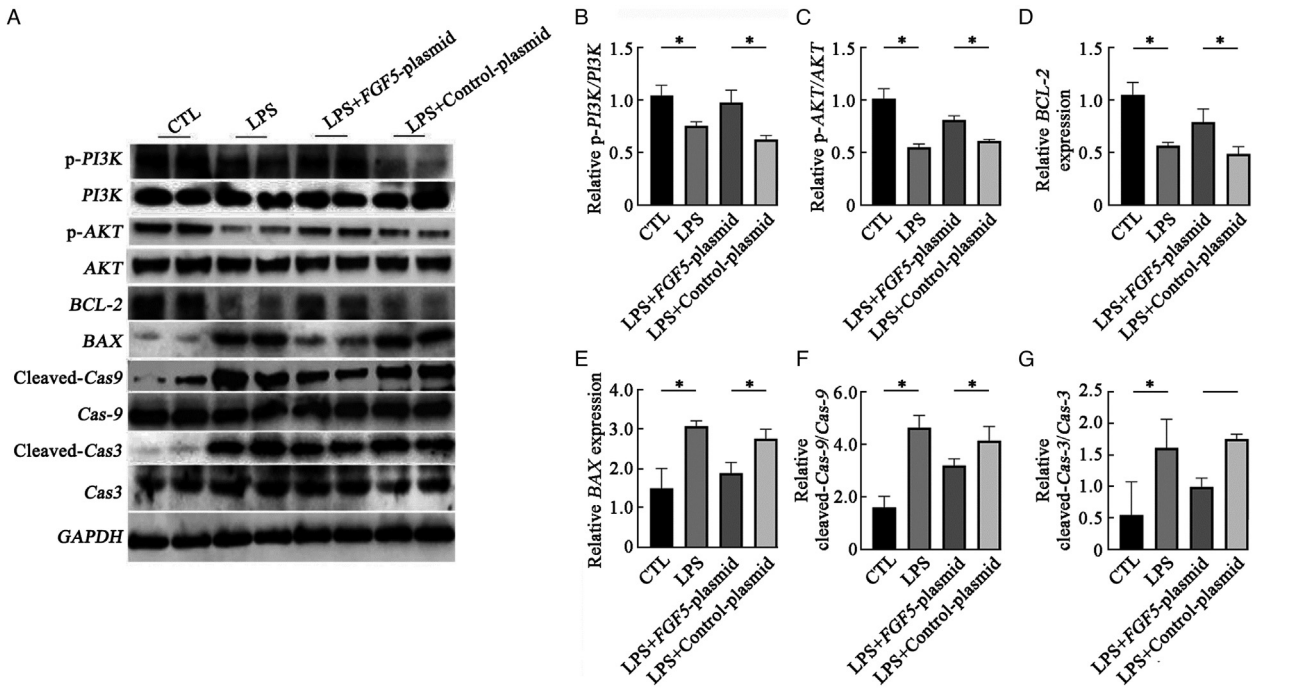

Figure 5: Fibroblast growth factor 5 (*FGF5*) overexpression exerts effects on the phosphoinositide-3-kinase/protein kinase B (PI3K/AKT*)* and apoptotic pathways *in vitro*: (A) Representative blot images. (B–G) The corresponding statistical analysis graphs ($n = 4$, $^{*}P < 0.05$). *BAX*: *BCL2*-associated X; *cas-3*: Caspase-3; *cas-9*: Caspase-9; CTL: Control group; *GAPDH*: Glyceraldehyde-3-phosphate dehydrogenase; LPS: Lipopolysaccharide; LPS + Ad-control group: LPS + adenovirus-control group; LPS + Ad-*FGF5*: LPS + adenovirus-*FGF5* group; p-*AKT*: Phosphorylated-protein kinase B; p-*PI3K*: Phosphorylated- phosphoinositide-3-kinase.

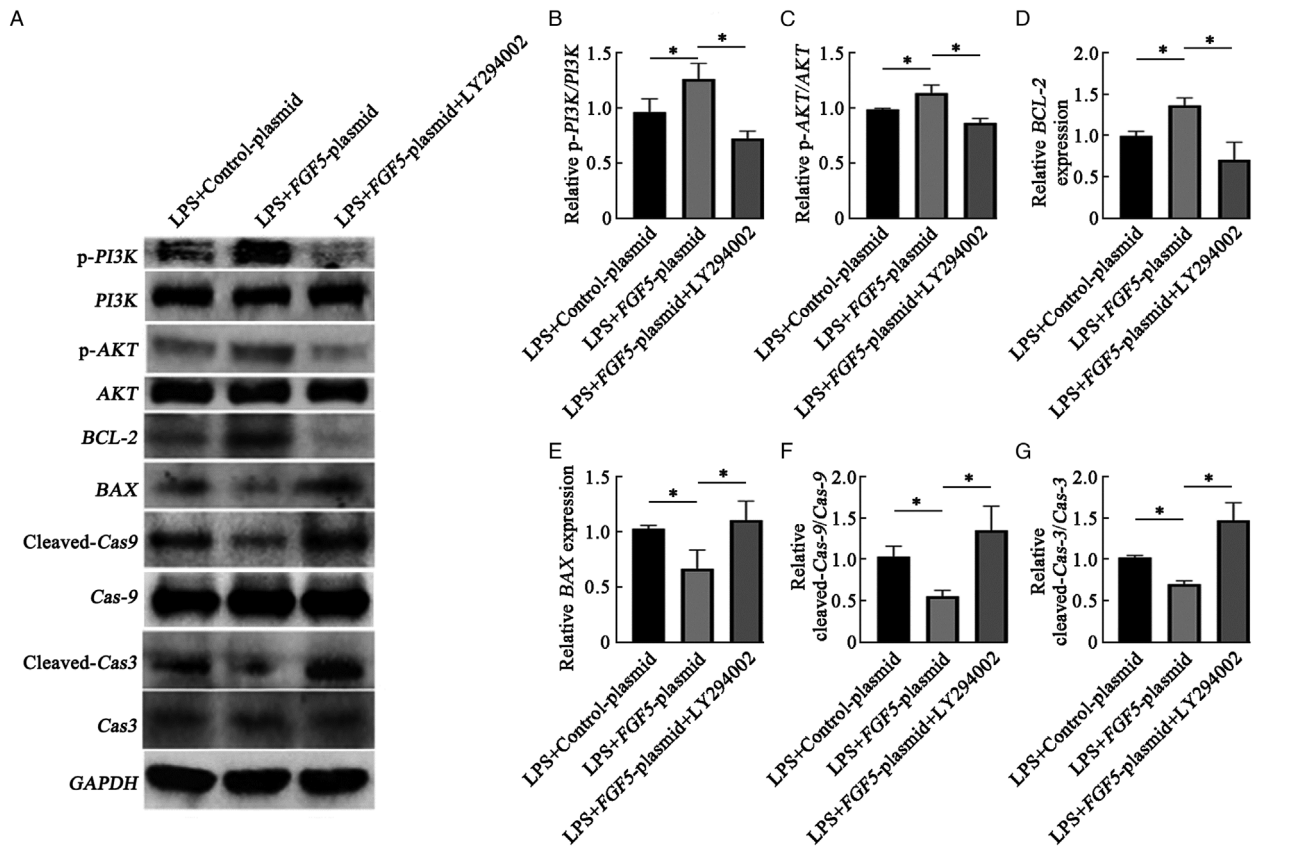

Figure 6: Fibroblast growth factor 5 (*FGF5*) protects hepatocytes against apoptosis by activating the phosphoinositide-3-kinase/protein kinase B (PI3K/AKT*)* pathway. (A) Representative blot images. (B–G): The corresponding statistical analysis graphs ($n = 3$, $^{*}P < 0.05$). *BAX*: *BCL2*-associated X; *cas-3*: Caspase-3; *cas-9*: Caspase-9; *GAPDH*: Glyceraldehyde-3-phosphate dehydrogenase; LPS: Lipopolysaccharide; p-*AKT*: Phosphorylated-protein kinase B; p-*PI3K*: Phosphorylated- phosphoinositide-3-kinase.

In conclusion, our current study demonstrated, for the first time, the anti-apoptotic effect of *FGF5* in hepatocytes and confirmed that the aforementioned protective effect of *FGF5* on LPS-induced hepatic injury depended on the activation of the PI3K/AKT signaling pathway, thus providing new insights for the clinical treatment of the septic liver injury.

Funding

This work was supported by the National Science and Technology Support Program (grant number: 2015BAI08B01).

Conflicts of interest

None.

References

1. Faix JD. Biomarkers of sepsis. Crit Rev Clin Lab Sci 2013;50:23–36. doi: 10.3109/10408363.2013.764490.
2. Sun J, Zhang J, Wang X, Ji F, Ronco C, Tian J, *et al*. Gut-liver crosstalk in sepsis-induced liver injury. Crit Care 2020;24:614. doi: 10.1186/s13054-020-03327-1.
3. Lelubre C, Vincent JL. Mechanisms and treatment of organ failure in sepsis. Nat Rev Nephrol 2018;14:417–427. doi: 10.1038/s41581-018-0005-7.
4. Yan J, Li S, Li S. The role of the liver in sepsis. Int Rev Immunol 2014;33:498–510. doi: 10.3109/08830185.2014.889129.
5. Beenken A, Mohammadi M. The FGF family: biology, pathophysiology and therapy. Nat Rev Drug Discov 2009;8:235–253. doi: 10.1038/nrd2792.
6. Zhang X, Ibrahimi OA, Olsen SK, Umemori H, Mohammadi M, Ornitz DM. Receptor specificity of the fibroblast growth factor family. The complete mammalian FGF family. J Biol Chem 2006;281:15694–15700. doi: 10.1074/jbc.M601252200.
7. Hui Q, Jin Z, Li X, Liu C, Wang X. FGF family: from drug development to clinical application. Int J Mol Sci 2018;19:1875. doi: 10.3390/ijms19071875.
8. Lee TW, Chung CC, Lee TI, Lin YK, Kao YH, Chen YJ. Fibroblast growth factor 23 stimulates cardiac fibroblast activity through phospholipase C-mediated calcium signaling. Int J Mol Sci 2021;23:166. doi: 10.3390/ijms23010166.
9. Wang J, Sontag D, Cattini PA. Heart-specific expression of FGF-16 and a potential role in postnatal cardioprotection. Cytokine Growth Factor Rev 2015;26:59–66. doi: 10.1016/j.cytogfr.2014.07.007.
10. Sofronescu AG, Detillieux KA, Cattini PA. FGF-16 is a target for adrenergic stimulation through NF-kappaB activation in postnatal cardiac cells and adult mouse heart. Cardiovasc Res 2010;87:102–110. doi: 10.1093/cvr/cvq025.
11. Balasubramanian R, Zhang X. Mechanisms of FGF gradient formation during embryogenesis. Semin Cell Dev Biol 2016;53:94–100. doi: 10.1016/j.semcdb.2015.10.004.
12. Yang L, Zhou F, Zheng D, Wang D, Li X, Zhao C, *et al*. FGF/FGFR signaling: from lung development to respiratory diseases. Cytokine Growth Factor Rev 2021;62:94–104. doi: 10.1016/j.cytogfr.2021.09.002.
13. Turner N, Grose R. Fibroblast growth factor signalling: from development to cancer. Nat Rev Cancer 2010;10:116–129. doi: 10.1038/nrc2780.
14. Giacomini A, Taranto S, Rezzola S, Matarazzo S, Grillo E, Bugatti M, *et al*. Inhibition of the FGF/FGFR system induces apoptosis in lung cancer cells via c-Myc downregulation and oxidative stress. Int J Mol Sci 2020;21:9376. doi: 10.3390/ijms21249376.
15. Zhao J, Lin H, Wang L, Guo K, Jing R, Li X, *et al*. Suppression of FGF5 and FGF18 expression by cholesterol-modified siRNAs promotes hair growth in mice. Front Pharmacol 2021;12:666860. doi: 10.3389/fphar.2021.666860.
16. Higgins CA, Petukhova L, Harel S, Ho YY, Drill E, Shapiro L, *et al*. FGF5 is a crucial regulator of hair length in humans. Proc Natl Acad Sci U S A 2014;111:10648–10653. doi: 10.1073/pnas.1402862111.
17. Zhang R, Li Y, Jia K, Xu X, Li Y, Zhao Y, *et al*. Crosstalk between androgen and Wnt/(-catenin leads to changes of wool density in FGF5-knockout sheep. Cell Death Dis 2020;11:407. doi: 10.1038/s41419-020-2622-x.
18. Hanaka H, Hamada T, Ito M, Nakashima H, Tomita K, Seki S, *et al*. Fibroblast growth factor-5 participates in the progression of hepatic fibrosis. Exp Anim 2014;63:85–92. doi: 10.1538/expanim.63.85.
19. Nakashima H, Nakashima M, Kinoshita M, Ikarashi M, Miyazaki H, Hanaka H, *et al*. Activation and increase of radio-sensitive CD11b+ recruited Kupffer cells/macrophages in diet-induced steatohepatitis in FGF5 deficient mice. Sci Rep 2016;6:34466. doi: 10.1038/srep34466.
20. Reddy SS, Chauhan P, Maurya P, Saini D, Yadav PP, Barthwal MK. Coagulin-L ameliorates TLR4 induced oxidative damage and immune response by regulating mitochondria and NOX-derived ROS. Toxicol Appl Pharmacol 2016;309:87–100. doi: 10.1016/j.taap.2016.08.022.
21. Xiong X, Ren Y, Cui Y, Li R, Wang C, Zhang Y. Obeticholic acid protects mice against lipopolysaccharide-induced liver injury and inflammation. Biomed Pharmacother 2017;96:1292–1298. doi: 10.1016/j.biopha.2017.11.083.
22. Hirano K, Shimizu Y, Nakayama Y, Minemura M, Yasumura S, Sugiyama T. Overexpression of granulocyte-macrophage colony-stimulating factor in mouse liver enhances the susceptibility of lipopolysaccharide leading to massive apoptosis of hepatocytes. Liver Int 2005;25:1027–1035. doi: 10.1111/j.1478-3231.2005.01136.x.
23. Liu H, Pathak P, Boehme S, Chiang JL. Cholesterol 7α-hydroxylase protects the liver from inflammation and fibrosis by maintaining cholesterol homeostasis. J Lipid Res 2016;57:1831–1844. doi: 10.1194/jlr.M069807.
24. Vázquez-Sánchez S, Poveda J, Navarro-García JA, González-Lafuente L, Rodríguez-Sánchez E, Ruilope LM, *et al*. An Overview of FGF-23 as a Novel candidate biomarker of cardiovascular risk. Front Physiol 2021;12:632260. doi: 10.3389/fphys.2021.632260.
25. Che J, Okigaki M, Takahashi T, Katsume A, Adachi Y, Yamaguchi S, *et al*. Endothelial FGF receptor signaling accelerates atherosclerosis. Am J Physiol Heart Circ Physiol 2011;300:H154–H161. doi: 10.1152/ajpheart.00075.2010.
26. Teven CM, Farina EM, Rivas J, Reid RR. Fibroblast growth factor (FGF) signaling in development and skeletal diseases. Genes Dis 2014;1:199–213. doi: 10.1016/j.gendis.2014.09.005.
27. Lin Q, Huang Z, Cai G, Fan X, Yan X, Liu Z, *et al*. Activating adenosine monophosphate-activated protein kinase mediates fibroblast growth factor 1 protection from nonalcoholic fatty liver disease in mice. Hepatology 2021;73:2206–2222. doi: 10.1002/hep.31568.
28. Song L, Wang L, Hou Y, Zhou J, Chen C, Ye X, *et al*. FGF4 protects the liver from nonalcoholic fatty liver disease by activating the AMP-activated protein kinase-Caspase 6 signal axis. Hepatology 2022;76:1105–1120. doi: 10.1002/hep.32404.
29. Zhu S, Ma L, Wu Y, Ye X, Zhang T, Zhang Q, *et al*. FGF21 treatment ameliorates alcoholic fatty liver through activation of AMPK-SIRT1 pathway. Acta Biochim Biophys Sin (Shanghai) 2014;46:1041–1048. doi: 10.1093/abbs/gmu097.
30. Gao Y, Zhang W, Zeng LQ, Bai H, Li J, Zhou J, *et al*. Exercise and dietary intervention ameliorate high-fat diet-induced NAFLD and liver aging by inducing lipophagy. Redox Biol 2020;36:101635. doi: 10.1016/j.redox.2020.101635.
31. Hua X, Sun DY, Zhang WJ, Fu JT, Tong J, Sun SJ, *et al*. P7C3-A20 alleviates fatty liver by shaping gut microbiota and inducing FGF21/FGF1, via the AMP-activated protein kinase/CREB regulated transcription coactivator 2 pathway. Br J Pharmacol 2021;178:2111–2130. doi: 10.1111/bph.15008.
32. Okada T, Enkhjargal B, Travis ZD, Ocak U, Tang J, Suzuki H, *et al*. FGF-2 attenuates neuronal apoptosis via FGFR3/PI3k/AKT signaling pathway after subarachnoid hemorrhage. Mol Neurobiol 2019;56:8203–8219. doi: 10.1007/s12035-019-01668-9.
33. Ronca R, Ghedini GC, Maccarinelli F, Sacco A, Locatelli SL, Foglio E, *et al*. FGF trapping inhibits multiple myeloma growth through c-Myc degradation-induced mitochondrial oxidative stress. Cancer Res 2020;80:2340–2354. doi: 10.1158/0008-5472.CAN-19-2714.

34. Linares GR, Leng Y, Maric D, Chuang DM. Overexpression of fibroblast growth factor-21 (FGF-21) protects mesenchymal stem cells against caspase-dependent apoptosis induced by oxidative stress and inflammation. Cell Biol Int 2020;44:2163–2169. doi: 10.1002/cbin.11409.
35. Hu L, Wang Y, Pan H, Kadir K, Wen J, Li S, *et al*. Apoptosis repressor with caspase recruitment domain (ARC) promotes bone regeneration of bone marrow-derived mesenchymal stem cells by activating Fgf-2/PI3K/AKT signaling. Stem Cell Res Ther 2021;12:185. doi: 10.1186/s13287-021-02253-5.
36. Yang S, Guo Y, Zhang W, Zhang J, Zhang Y, Xu P. Effect of FGF-21 on implant bone defects through hepatocyte growth factor (HGF)-mediated PI3K/AKT signaling pathway. Biomed Pharmacother 2019;109:1259–1267. doi: 10.1016/j.biopha.2018.10.150.
37. Xi B, Shen Y, Reilly KH, Wang X, Mi J. Recapitulation of four hypertension susceptibility genes (CSK, CYP17A1, MTHFR, and FGF5) in East Asians. Metabolism 2013;62:196–203. doi: 10.1016/j.metabol.2012.07.008.
38. Jeong H, Jin HS, Kim SS, Shin D. Identifying interactions between dietary sodium, potassium, sodium-potassium ratios, and FGF5 rs16998073 variants and their associated risk for hypertension in Korean adults. Nutrients 2020;12:2121. doi: 10.3390/nu12072121.
39. Ren Y, Jiao X, Zhang L. Expression level of fibroblast growth factor 5 (FGF5) in the peripheral blood of primary hypertension and its clinical significance. Saudi J Biol Sci 2018;25:469–473. doi: 10.1016/j.sjbs.2017.11.043.
40. Li J, Shi J, Huang W, Sun J, Wu Y, Duan Q, *et al*. Variant near FGF5 has stronger effects on blood pressure in Chinese with a higher body mass index. Am J Hypertens 2015;28:1031–1037. doi: 10.1093/ajh/hpu263.
41. Oh HN, Lee MH, Kim E, Kwak AW, Yoon G, Cho SS, *et al*. Licochalcone D induces ROS-dependent apoptosis in gefitinib-sensitive or resistant lung cancer cells by targeting EGFR and MET. Biomolecules 2020;10:297. doi: 10.3390/biom10020297.
42. Fresno Vara JA, Casado E, de Castro J, Cejas P, Belda-Iniesta C, González-Barón M. PI3K/AKT signalling pathway and cancer. Cancer Treat Rev 2004;30:193–204. doi: 10.1016/j.ctrv.2003.07.007.
43. Shariati M, Meric-Bernstam F. Targeting AKT for cancer therapy. Expert Opin Investig Drugs 2019;28:977–988. doi: 10.1080/13543784.2019.1676726.
44. Zhou BH, Tan PP, Jia LS, Zhao WP, Wang JC, Wang HW. PI3K/AKT signaling pathway involvement in fluoride-induced apoptosis in C2C12 cells. Chemosphere 2018;199:297–302. doi: 10.1016/j.chemosphere.2018.02.057.
45. Wu Y, Ma J, Sun Y, Tang M, Kong L. Effect and mechanism of PI3K/AKT/mTOR signaling pathway in the apoptosis of GC-1 cells induced by nickel nanoparticles. Chemosphere 2020;255:126913. doi: 10.1016/j.chemosphere.2020.126913.
46. Sheta M, Hassan G, Afify SM, Monzur S, Kumon K, Abu Quora HA, *et al*. Chronic exposure to FGF2 converts iPSCs into cancer stem cells with an enhanced integrin/focal adhesion/PI3K/AKT axis. Cancer Lett 2021;521:142–154. doi: 10.1016/j.canlet.2021.08.026.
47. Labrèche C, Cook DP, Abou-Hamad J, Pascoal J, Pryce BR, Al-Zahrani KN, *et al*. Periostin gene expression in neu-positive breast cancer cells is regulated by a FGFR signaling cross talk with TGF (/PI3K/AKT pathways. Breast Cancer Res 2021;23:107. doi: 10.1186/s13058-021-01487-8.
48. Even-Chen O, Barak S. Inhibition of FGF receptor-1 suppresses alcohol consumption: Role of PI3 kinase signaling in dorsomedial striatum. J Neurosci 2019;39:7947–7957. doi: 10.1523/JNEUROSCI.0805-19.2019.

How to cite this article: Cui S, Li Y, Zhang X, Wu B, Li M, Gao J, Xu L, Xia H. Fibroblast growth factor 5 overexpression ameliorated lipopolysaccharide-induced apoptosis of hepatocytes through regulation of the phosphoinositide-3-kinase/protein kinase B pathway. Chin Med J 2022;135:2859–2868. doi: 10.1097/CM9.0000000000002540